J. Enzyme Inhibition, 1997, Vol. 12, pp. 101–121
Reprints available directly from the publisher
Photocopying permitted by license only

YEAST HEXOKINASE INHIBITORS DESIGNED FROM THE 3-D ENZYME STRUCTURE REBUILDING

MICHELE WILLSON[a,*], ISABELLE ALRIC[a],
JACQUES PERIE[a] and YVES HENRI SANEJOUAND[b]

[a] *Groupe de Chimie Organique Biologique, IMRCP UMR-CNRS 5623;*
[b] *Laboratoire de Physique Quantique, IRSAMC UMR-CNRS 505,*
Université Paul Sabatier, 118 route de Narbonne, 31 062 Toulouse Cedex, France

(Received 4 November 1996; In final form 25 January 1997)

This work describes a search for hexokinase inhibitors based on the interactions analysis at the active site of the X-ray resolved *o*-tolulyl-glucosamine-hexokinase (OTG-HK) complex structure. As the actual enzyme sequence was unknown when the X-ray structure was made (only 30% homology), the structure of the complex was rebuilt by modelling on the X-ray structure frame which allowed residues in close vicinity to the inhibitor to be defined, particularly Glu249 and Gln278. Compounds with inhibitor-bearing groups able to interact with these residues were synthesized and assayed. Some of them revealed strong affinities, in the Km range for glucose. Kinetic analysis of their behaviour towards glucose and ATP together with spectroscopic studies using NMR, allowed the determination of the corresponding inhibition patterns and provided complementary information on HK.

Keywords: Hexokinase; Enzyme structure rebuilding; Inhibitors; Kinetics; NMR spectroscopy

ABBREVIATIONS

HK – hexokinase, EC 2.7.1.1; OTG – *o*-tolulyl-glucosamine; ATP – adenosine triphosphate; ADP – adenosine diphosphate; G6PDH – Glucose-6-phosphate dehydrogenase; PyK – pyruvate kinase; LDH – lactate dehydrogenase; PEP – phospho-enol-pyruvate; TEA – triethanolamine.

* Corresponding author. Fax: 05 61 25 17 33; E-mail. willson@iris.ups-tlse.fr.

INTRODUCTION

In the search for inhibitors of glycolytic enzymes[1,2] we have focused our research on hexokinase (HK), the first enzyme in the Embden-Meyerhoff pathway, which transforms glucose into glucose-6-phosphate. This enzyme is of prime importance since it is involved in glycolysis, in the pentose-phosphate pathway for the synthesis of nucleic acids and may be involved in glucose import. It is known, for example, that in some bacteria, glucose import is associated with a phosphorylation process;[3] in yeast also, three kinases play a role in hexose uptake by binding to the carriers.[4]

Glycolysis is an important target in the development of new anti-parasitic drugs. It is well known that in protozoan parasites such as trypanosomes, this metabolism is essential since glucose represents their only source of energy.[5] Therefore the development of efficient inhibitors for enzymes of this pathway may lead to biologically active molecules, and, hopefully, to the development of new drugs against the diseases that these parasites are responsible for.[6]

The search for inhibitors of hexokinase (from bovine brain, rabbit muscle or human) has not been very successful so far. The inhibitors for yeast HK previously described in the literature belong to three groups of compounds: (1) deoxy derivatives of hexoses (glucose, mannose and galactose) which give weak inhibitions in the millimolar range with no specific effect at high pH values,[7,8] (2) hexoses-6-phosphate analogues which inhibit human hexokinase I by interacting at regulatory sites,[9,10] (3) bisubstrates inhibitors, where the glucose moiety is bound through a spacer to an ATP analogue and which have an inhibition constant in the range of 1 to 2.5 mM.[11] In our own research for inhibitors of hexokinases from yeast and *Trypanosoma brucei*, glucose-6-phosphate analogues also revealed weak inhibition.[12] Subsequently, a similar work has been published by Coats *et al.*[22] but the results obtained by these authors are questionable.

These rather disappointing results may be related to the large conformational change that hexokinases A or B undergo during their catalytic cycle. Such a change has been revealed by X-ray analysis where two structures, one in a closed conformation with a glucose molecule bound at the active site[13,14] the other in an open conformation without substrate[15,16] have been characterized. A reasonable assumption is that affinities of glucose analogues will depend on how these structures block or accommodate such conformational changes.

An example is given by the glucose analogue N-(*o*-acetylaminobenzoyl)-D-glucosamine (OTG), an inhibitor with a K_i value of 1 mM for the yeast

enzyme[17,18] which has been co-crystallized with hexokinase and for which the X-ray structure indicates an open form for the enzyme.[19] Through the X-ray structure of the OTG-hexokinase complex, the inhibitor position at the glucose binding site can be determined. However the analysis of the specific interactions between the inhibitor and the protein is not very informative because this structure was published before the sequence of the yeast hexokinase was known;[20] as a consequence, there are numerous errors in the crystallographic structures of hexokinase at the residue level.

To get a better insight into the actual interactions between hexokinase and OTG, which was used as a reference, we had to rebuild the structure of the complex, by inserting its own amino-acid sequence. This modeling is in good agreement with different literature data (see discussion). From the analysis of the rebuilt complex, and particularly the nature of residues lying in the vicinity of the aromatic ring of OTG, we have designed a new set of molecules closely related in structure to OTG, and therefore corresponding to this model, which were synthesized and investigated as hexokinase inhibitors using kinetic methods and NMR spectroscopy.

MATERIALS AND METHODS

Source of Enzymes, Subtrates and Cofactors

Yeast hexokinase, glucose, ATP, NADH, $NADP^+$, phospho-enol-pyruvate, glucose-6-phosphate-dehydrogenase (G6PDH), pyruvate-kinase (PyK) and lactate-dehydrogenase (LDH) were purchased from Boehringer, Mannheim (Germany).

Assay of Enzyme Activities

The phosphotransferase activity was followed spectrophotometrically by reduction of $NADP^+$ in the presence of an excess of glucose-6-phosphate-dehydrogenase (as described in method A). ATPase activity was measured by spectrophotometric measurement of the rate of oxidation of NADH in the presence of phospho-enol-pyruvate, pyruvate-kinase and lactate-dehydrogenase (method B)

Method A:

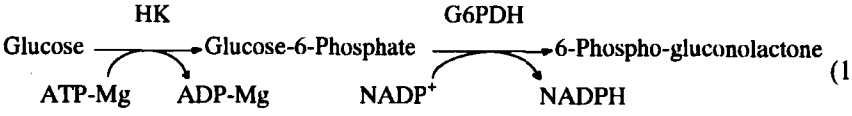

(1)

Method B:

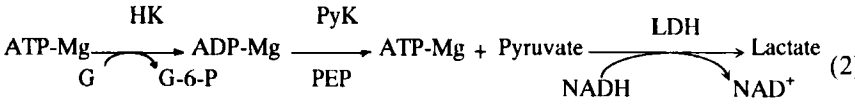

(2)

Inactivation Studies

The inactivation of HK by the different compounds was measured in the direction of NADPH (method A) or NAD^+(method B) formation; their concentrations were calculated from their absorbance using $\varepsilon_{340} = 6.22\,mM^{-1}\,cm^{-1}$. All reactions were carried out at 25°C and the formation of NADPH or NAD^+ at 340 nm was measured with a Perkin Elmer spectrophotometer equipped with a kinetic accessory unit. The activities of the compounds on HK were measured after preincubation of the enzyme with the compound in the assay buffer for 5 min followed by the addition of the reaction mixture to trigger off the reaction. Initial slopes were measured for the first 3 min of the reaction.

In method A, for phospho-transferase activity, the reaction mixture (1 mL) contained 0.1 M triethanolamine hydrochloride buffer (pH 7.6), 1 mM EDTA, 0.64 mM $NADP^+$, 0.66 mM ATP, 10 mM $MgCl_2$, 10 mM glucose and 5 μg G6PDH (0.7 unit).

In method B, for assaying formation of ADP-Mg, the reaction mixture (1 mL) contained 0.1 M triethanolamine hydrochloride buffer (pH 7.6), 1 mM EDTA, 0.42 mM NADH, 2.5 mM PEP, 0.66 mM ATP, 10 mM $MgCl_2$, 2.5 μL of 1/1 PyK/LDH (1.1 unit).

Possible effects of the inhibitors on the absorbance of NADPH or NADH were checked by running enzyme free blank reactions. The remaining activity was determined from comparison with the control experiment in which the inhibitor was replaced by the same amount of solvent dimethylsulfoxide (DMSO). At a concentration of solvent below 10%, no significant effect on the enzyme activity was observed. The concentration of inhibitor required for 50% inhibition (IC50) was calculated from at least 5 inhibitor concentrations that were tested at saturating conditions of substrate. The type of inhibition and the inhibition constant (K_i) were determined from Lineweaver-Burk plots.

The inhibition with respect to glucose was studied at three different concentrations of glucose (100 μM, 200 μM and 300 μM) at saturating concentration of ATP (0.66 mM). The inhibition with respect to ATP was studied at three different concentrations of ATP (0.22 mM, 0.33 mM and 0.44 mM) at saturating concentration of glucose (10 mM).

Nuclear Magnetic Resonance

Nuclear Magnetic Resonance (NMR) experiments were carried out using a Bruker Fourier transform 31P NMR spectrometer operating at 110 MHz. Sample volumes of 1 mL in 5 mm diameter tubes were used with 85% phosphoric acid as reference. The test tube initially contained 10 mmoles of inhibitor in 100 μL of DMSO, 20 μmoles of ATP-Mg in 400 μL of buffer (TEA pH 7.6) and 0.5 mg of HK. Experiments were run in triplicate and with control experiments under the same conditions without enzyme. Chemical shifts were ascribed to the different products (ADP, AMP and Pi) by comparison with authentic samples.

Molecular Modeling

The molecular modeling software used was QUANTA version 3.2 (Polygen corp.). Crystal structures used are identified in the Protein Data Bank as 2yhx for the open form and as 1hkg for the closed form of Yeast Hexokinase. The model OTG in the closed form, was built following Benett and Steitz[14] protocol; the glucose binding sites (residues 1–57 and 186–457) of both forms were superimposed using a least square fit algorithm. No rotamer search was performed because the original crystallographic model is so incomplete that it may contain sizeable inaccuracies and should not be regarded as a true 2.1 Å resolution structure.

Synthesis of N-amido Glucosamine Derivatives

The pure compounds were identified by spectrometric analysis. IR spectra were recorded on a Perkin-Elmer FTIR 1610 spectrometer, ^{1}H and ^{13}C NMR spectra were run on a Bruker 250MHZ FT apparatus and mass spectra were performed on a Nermag R10-10.

The general procedure for the synthesis of this set of compounds was by coupling the appropriate anhydrides to the glucosamine under stoichiometric conditions at room temperature in methanol–water or dimethylsulfoxide after neutralisation of the glucosamine hydrochloride by carbonated resin Dowex 5×8 (in methanol–water) or by tertiary organic basis (in DMSO). The products were precipitated by addition of methanol or methylene chloride and were purified by recrystallization from a large volume of ethanol. The *o*- and *p*- amino compounds were synthesized from the nitro analogues by catalytic reduction on Pd/C in methanol.

Atom numbering is given in Table I.

N-benzoyl-D-glucosamine 1

Yield = 90%. TLC (eluent ethanol) Rf = 0.8. IR (pellet Kbr) νcm^{-1}: 1632 (C=O). ^{1}H-NMR (DMSO) δ (ppm), 6.45 (d, C_1H, J = 4.5 Hz), 6.54 (d, NH, J = 6.25 Hz). ^{13}C-NMR (DMSO) δ (ppm) (forms α and β): 55.24-57.46 (C2), 61.04-61.06 (C6), 69.95-70.94 (C3), 70.92-72.04 (C4), 74.05-76-79 (C5), 90.32-95.27 (C1), 127.12-128.34 (C*4-C*6), 127.21-127.33 (C*3-C*1), 130.61-131.01 (C*5), 134.38-134.97 (C*2), 166.25-166.34 (C*8). Mass: (FAB), MH^+, 284; MNa^+, 306.

N-(o-bromobenzoyl)-D-glucosamine 3

Yield = 50%. TLC (eluent ethanol) Rf = 0.75. IR (pellet) νcm^{-1} 1630 (C=O). ^{1}H NMR (DMSO) δ (ppm) 4.52 (d, C1H, J = 7.5 Hz), 5.10 (d, NH, J = 5 Hz). ^{13}C NMR (DMSO) δ (ppm) (α and β forms): 55.12-57.42 (C2), 61.05 (C6), 69.76-70.82 (C3), 70.98-73.96 (C4), 72.04-76.85 (C5), 90.31-95.34 (C1), 119.03 (C*1), 127.14 (C*4), 130.64-129-24 (C*3), 132.52 (C*6), 132.66-133.40 (C*5), 138.78-139.23 (C*2), 167.12-167.21 (C*8). Mass: (FAB), MH^+, 361; MNa^+, 384.

N-(o-N'-acetylaminobenzoyl)-D-glucosamine 4

Yield = 45%. TLC (eluent ethanol) Rf = 0.7. IR (pellet) νcm^{-1} 1642 (C*8=O), 1648 (C*7=O). ^{13}C NMR (DMSO) δ(ppm) (α form): 24.8 (C*9), 54.43 (C2), 54.76 (C6), 69.70 (C3), 72.23 (C5), 77.12 (C4), 88.6 (C1) 115.85 (C*1), 119.71 (C*6), 122.36 (C*4), 130.92 (C*3), 133.58 (C*5), 140.75 (C*2), 166.29 (C*8), 169.42 (C*7). Mass: (FAB), MH^+, 341.

N-(o-carboxybenzoyl)-D-glucosamine 5

Yield = 56%. TLC (eluent ethanol) Rf = 0.45. IR (pellet) νcm^{-1} 1643 (C*8=O), 1714 (C*7=O). ^{13}C NMR (DMSO) δ (ppm) (α form): 54.91 (C2), 61.03 (C6), 70.38 (C3), 70.73 (C4), 72.03 (C5), 90.48 (C1), 127.93 (C*3), 128.85 (C*6), 129.11 (C*5), 130.79 (C*4), 130.92 (C*1), 137.96 (C*2). Mass: (FAB), MH^+, 328.

N-pyrazinyl-D-glucosamide 6

Yield = 60%. TLC (eluent ethanol) Rf = 0.75. IR νcm^{-1} (pellet) 1640 (C*8=O). ^{13}C NMR (DMSO) δ (ppm) (forms α and β): 54.41-56.24 (C2), 60.92-61.50 (C6), 70.49-70.73 (C3), 70.60-73.52 (C4), 72.34-76.21 (C5),

90.36-95.34 (C1), 143.12-143.21 (C*3, C*4), 147.30 (C*2), 144 (C*1), 166.22 (C*8). Mass: (FAB), MH^+, 285.

N-(o-nitrobenzoyl)-D-glucosamine 7

Yield = 80%. TLC (eluent ethanol) Rf = 0.80. IR νcm^{-1} (pellet) 1645 (C*8=O), 1550-1395 (NO_2). ^1H NMR δ (ppm) 6.50 (d, C1H, J = 5 Hz), 6.63 (d, NH, J = 6.25 Hz). ^{13}C NMR (DMSO) δ (ppm) (forms α and β): 54.95-58.60 (C2), 60.98 (C6), 70.03-70.80 (C3), 70.94-72.09 (C4), 72.00-74.24 (C5), 90.27-94.82 (C1), 123.69-123.42 (C*6), 129.43-130.10 (C*3), 130.50-130.90 (C*4), 132.31-132 (C*2), 133.03-132.40 (C*5), 147.15-147.80 (C*1), 165.49-164.22 (C*8). Mass: (FAB), MH^+, 239.

N-(m-nitrobenzoyl)-D-glucosamine 8

Yield = 80%. TLC (eluent ethanol) Rf = 0.80. IR νcm^{-1} (pellet): 1640 (C*8=O), 1560-1405 (NO_2). ^1H NMR (DMSO) δ (ppm): 6.52 (d, C1H, J = 5.5 Hz), 6.65 (d, NH, J = 6.25 Hz). ^{13}C NMR (DMSO) δ (ppm) forms α and β): 55.50-57.65 (C2), 60.96 (C6), 69.85-70.64-70.90-72.00 (C3, C4), 73.97-76.82 (C5), 90.23-95.04 (C1), 121.77-122.17 (C*1), 125.53-125.65 (C*5), 129.82-130 (C*4), 133.80-133.97 (C*3), 135.79-136.38 (C*2), 147.52 (C*6), 164.03-164.40 (C*8). Mass: (FAB), MH^+, 329.

N-(o aminobenzoyl)-D-glucosamine 9

Yield = 70%. TLC (eluent ethanol) Rf = 0.65. IR νcm^{-1} (pellet) 1648 (C*8=O). ^1H NMR (DMSO) δ (ppm): 6.50 (d, C1H, J = 5 Hz), 6.56 (d, NH, J = 6 Hz). ^{13}C NMR (DMSO) δ (ppm) (form α): 54.77 (C2), 61.05 (C6), 69.99 (C3), 70.85 (C4), 72.06 (C5), 90.36 (C1), 114.44 (C*6), 114.93 (C*2), 116.11 (C*4), 128.42 (C*3), 131.50 (C*5), 149.28 (C*1), 168.78 (C*8). Mass: (FAB), MH^+, 299.

N-(m-aminobenzoyl)-D-glucosamine 10

Yield = 40%. TLC (eluent ethanol) Rf = 0.65. IR νcm^{-1} (pellet) 1645 (C*8=O). ^1H NMR (DMSO) δ (ppm): 6.49 (d, C1H, J = 5 Hz), 6.52 (d, NH, J = 6 Hz). ^{13}C NMR (DMSO) δ (ppm) (forms α and β): 55.09-55.92 (C2), 61.02 (C6), 69.96-70.80 (C3), 70.80-72.80 (C4), 74.02-76.74 (C5), 90.31-95.28 (C1), 112.81-113.06 (C*1), 114.24-114.59 (C*3), 116.22-116.40 (C*5), 128.28-128.46 (C*4), 135.27-135.50 (C*2), 148.13-148.26 (C*6), 166.70-166.91 (C*8). Mass: (FAB), MH^+, 299.

RESULTS

Modeling Studies

As indicated above, the hexokinase A and B sequences were not available at the time the corresponding crystal structure was obtained. Comparison of the sequence found by X-ray studies with the actual amino-acid sequence revealed only a 30% identity. After alignment of the yeast hexokinase B sequence with the crystallographic sequence (Figure 1), the open and closed forms were rebuilt according to the following protocol. For every residue where the crystallographic data was in agreement with the actual sequence information, the atoms were located according to the crystallographic data; additonal atoms, found in the correct residues and not in the crystallographic data, were positioned according to topological information only (known average bond lengths, valence angle values, etc...). In particular, no attempt was made to energy-minimize the structures obtained; thus these structures are as close as possible to the experimental X-ray data.

The positioning of the inhibitor OTG atoms in the closed form was performed following the route used by Bennett and Steitz[14] (for positioning the glucose ring in the closed form). According to these authors, the glucose ring position is the same in the open and the closed forms, with respect to the large lobe of hexokinase. The closed structure of the OTG-HK complex will be referred to as the "hypothetical structure".

Figures 2 and 3 indicate all heavy atoms present in the rebuilt structures at distances from OTG inferior to 5 Å (names and numbering of residues are indicated under each oxygen or nitrogen atom). The numbering of residues starts at position 20 of that given by Fothergill-Gilmore and Michels.[21] This numbering is close but different to that given by Steitz *et al.* The distances indicated by broken lines are those inferior to 3.5 Å.

A detailed analysis of these interactions is given in Tables I and II with the listing of Van der Waals contacts and hydrogen bonds between the protein and the toluyl moiety and between the protein and the carbohydrate moiety, in both open and closed conformations of hexokinase. From the binding-site topologies, definite patterns and trends emerge in connection with inhibition constants and with the most probable mode of inhibitor binding described in this work.

Van der Waals Contacts

Concerning the contacts between protein and carbohydrate moiety: for the open form and closed conformations of hexokinase, there are respectively

FIGURE 1 Alignment of the yeast hexokinase sequence Yeab[20] with the inferred crystallographic sequence 2yhx[19,15] using the FASTA algorithm. Amino acids denoted X were given as being "unknown" by the crystallographers. A "*" has been put under residues when some of their atoms were found within 5 Å of OTG, either in the closed or in the open form of hexokinase.

34 and 44 Van der Waals interactions corresponding to distances inferior to 4 Å. There are about the same number (20 to 21) of contacts involving distances between 3 and 3.8 Å, but several of these contacts are not entirely equivalent since different residues are involved in the contact between the protein and the carbohydrate moiety in the two conformations.

(i) For the open conformation, the Van der Waals contacts are confined to aminoacid residues of the large lobe located between positions 190 and 282. (ii) As expected, in the closed conformation, there are also contacts with amino acid residues of the small lobe: Ser 138 and Phe 139, the atom Oγ of the former being at an equal distance from the C-5, C-6 and O-5 atoms of the glucose ring.

Table I lists the contacts between the toluyl moiety of OTG and the protein. (i) In the open form, only Glu 249 and Gln 278, in the large lobe, make contacts (3.4 to 2 Å) with carbon atoms of the aromatic ring (ii) In the closed form, the structure of the hypothetical OTG complex suggests many possible contacts with residue Thr 155 of the small lobe and a tight

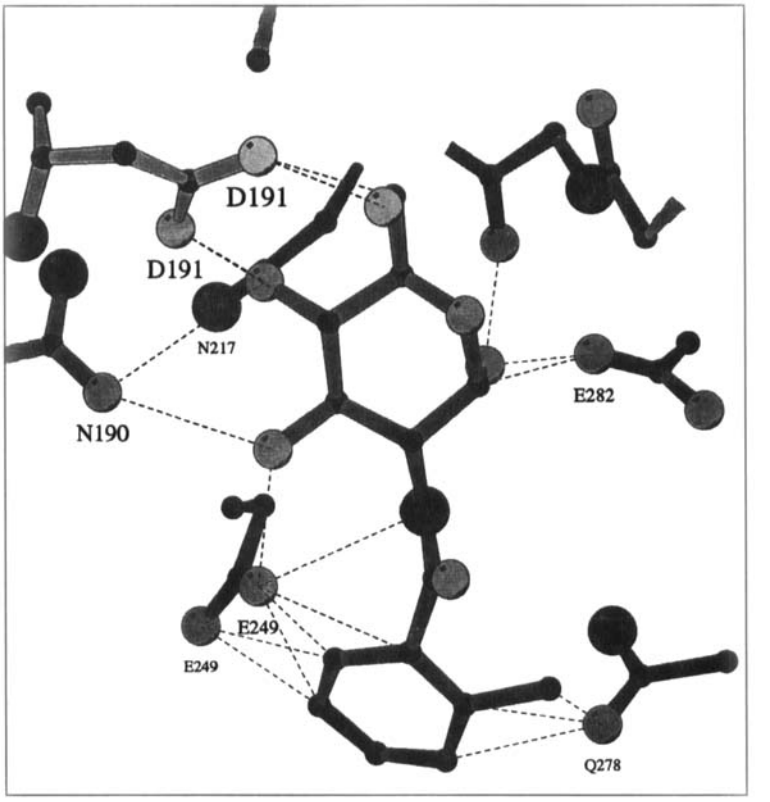

FIGURE 2 Active site of hexokinase with the OTG inhibitor bound to the open form after rebuilding performed (see text). The starting coordinates were obtained from the Brookhaven Protein Data Bank. Dashed lines indicate distances shorter than 3.5 Å. This picture was prepared using the Molscript program[34] (see Color Plate I).

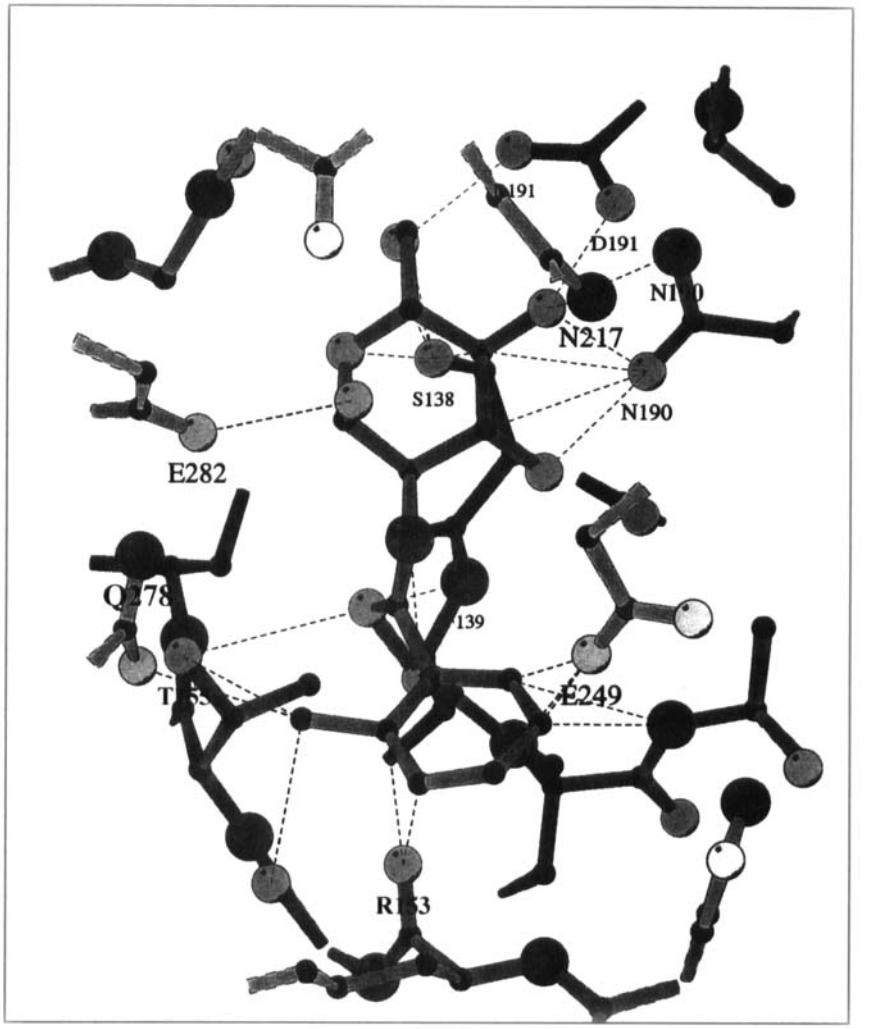

interaction with carbonyl groups of the peptide chain at residues Phe 139 and Arg 153. Note that very unfavored contacts are rare.

Hydrogen Bonds

An important difference is observed in the hydrogen bonding patterns between glucosamine and HK in the two conformations (Table II). (i) In

TABLE I Van der Waals interactions between the *o*-toluyl part of OTG and hexokinase in open form (from X-ray) and closed form (from model building) (b = backbone). The numbers and asterisks on carbon atoms are those from the protein data bank[19]

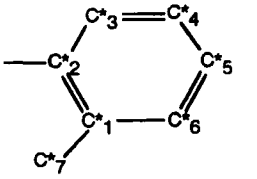

	Open Form		*Closed Form*	
Toluyl atoms	*Contacts* < 4 Å	*Distances* Å	*Contacts* < 4 Å	*Distances* Å
			b-Phe139 (CO)	3.02
C*1	Gln218 (O1)	3.39	b-Arg153 (CO)	3.95
			b-Trp154 (CO)	3.69
C*2	Glu249 (O1)	3.08	Glu249 (O1)	3.67
			b-Phe139 (CO)	2.21
C*3	Glu249 (O1)	1.94	Glu249 (O1)	2.62
			Pro140 (N)	3.63
			b-Ala141 (N)	3.31
			b-Phe139 (CO)	2.85
C*4	Glu249 (O1)	2.36	Glu249 (O1)	1.88
			Glu249 (O2)	3.91
			b-Ala141 (N)	3.41
C*5			Glu249 (O1)	2.75
C*6	Gln278 (O1)	3.14	b-Arg153 (CO)	2.98
C*7	Gln218 (O1)	2.89	Gln278 (O1)	3.39
			Thr155 (Cβ)	2.66
			Thr155 (Cγ)	2.86
			Thr155 (O1)	3.20
			b-Trp154 (CO)	3.29
			b-Phe139 (CO)	3.62
			b-Arg153 (CO)	3.60

the closed conformation, all the hydroxyl groups of the sugar behave simultaneously as hydrogen bond donors and acceptors; this cooperative effect is known to lead to stronger than average hydrogen bonds. The OH-6 is tightly associated with Ser 138 located on the small lobe (distance less than 2.5 Å) and has strong contacts with Asp 191. C-4 and O-4 atoms of the sugar have strong contacts with residues Ser 138 and Asp 191. (ii) In the open conformation the OH-6 is essentially associated with Asp 191 (distance less than 2.5 Å) from the large lobe, without any contact with Ser 138. Moreover, the amide bond on the C-2 of the sugar has interactions with the backbone in the small lobe, the oxygen O-8 and the nitrogen N-2 of this amide bond being associated with N-H and C=O groups at the Phe 139.

TABLE II Hydrogen bonds between the glucosamine part of OTG and hexokinase. Hydrogen bonds between the amide group N2–C*8=O*8 and hexokinase in the closed form (from model building)

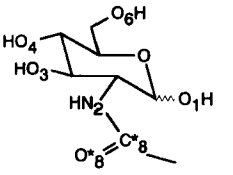

Open Form			*Closed Form*		
Donors (X)	*Acceptors (Y)*	*X–Y (Å)*	*Donors (X)*	*Acceptors (Yx)*	*X–Y (Å)*
O1	Glu282(O1)	2.02	O1	Glu282(O1)	3.03
O3	Glu249(O1)	3.03			
O4	Asp191(O)	2.56	O4	Asn190(O)	2.34
O6	Asp191(O)	2.42	O6	Asp191(O)	3.01
			O6	Ser138(O)	2.42
			Asn190(NH_2)	O3	2.67
			Asn190(NH_2)	O4	2.55
			N_2	b-Phe139(CO)	3.29
			b-Phe139(NH)	O*8	3.35
			Lys156(NH)	O*8	3.70

Inhibitor Molecules

The results of this modeling, by alignment of its own protein sequence on the X-ray structure and especially the nature of the residues lying in the vicinity of the ortho and meta positions (no contact with the para position) on the aromatic ring, Glu 249 and Gln 278 residues, were taken into account for the design of a new set of inhibitors. Groups able to promote hydrogen bonding or electrostatic interactions with these residues in particular were considered. The following compounds were synthesized and investigated:

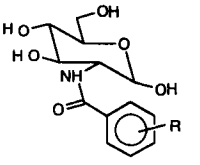

1, R = H;
2, *o*-CH_3;
3, *o*-Br;
4, *o*-$NHCOCH_3$;
5, *o*-COOH;
6, Pyrazinyl;
7, *o*-NO_2;
8, *m*-NO_2;
9, *o*-NH_2;
10, *m*-NH_2.

TABLE III Inhibition values for glucosamine derivatives on yeast hexokinase

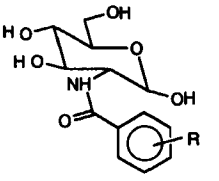

R		*IC50* (mM)[†]
H	**1**	7
o-CH_3	**2**	8
o-Br	**3**	—
o-$NHCOCH_3$	**4**	18
o-COOH	**5**	—
Pyrazinyl	**6**	20
o-NO_2	**7**	3
m-NO_2	**8**	6
o-NH_2	**9**	1
m-NH_2	**10**	6

[†](—) no activity at 20 mM. Each determination is done in triplicate with S.D ± 4%.

Two of these compounds (**1** and **8**) have been previously described by Coats *et al.* and assayed on yeast hexokinase.[22] But since some of the results obtained by these authors were at significant variance with ours,[23] we chose to use these compounds as a reference. Inhibition values (IC50) are given in Table III and were determined by the same kinetic method as used by the authors above (described in experimental methods). They indicate that the best results are obtained with N-aryl glucosamines bearing polar groups at the ortho or meta position, except for compound **5**.

Inactivation Kinetics

This study was performed for several reasons. Firstly, it was necessary to define accurately the inactivation process, because hexokinase is an enzyme where conformational fluctuations play a role in kinetic behavior[24] and, secondly, because the inhibitors investigated are susceptible to acting as alternative substrates, accounting for the discrepancy between Coat's results and ours.

(a) With respect to Glucose (results are given in Table IV)

For compounds **1**, **9** and **10**, the Lineweaver reciprocal plots (1/v versus 1/Glucose) intersect on the 1/v axis, at any concentration of the inhibitor. These three compounds clearly compete for the glucose substrate, the best

TABLE IV Inhibition patterns for inhibitors with Hexokinase as analyzed by Dixon plots using methods A and B (see text)

Compounds		*With respect to Glucose (method A)*†	*With respect to* ATP *(method A)*†	*Inhibitor as substrate* [10 mM] *Formation of* ADP (%) *with respect to* G [10 mM] *(method B)*
H	**1**	C $K_i = 1000\,\mu M$	U	5%
o-NO_2	**7**	MT $K_i = 500\,\mu M$ $K_{ii} = 900\,\mu M$	P-NC	28%
m-NO_2	**8**	MT $K_i = 450\,\mu M$ $K_{ii} = 800\,\mu M$	Non-linear	9%
o-NH	**9**	C $K_i = 280\,\mu M$	P-NC	34%
m-NH	**10**	C $K_i = 200\,\mu M$	Non-linear	15%

†C, competitive; MT, mixed type; U, uncompetitive; P-NC, partially non-competitive.

K_i values (200 and 280 μM) being obtained with the amino substituted compounds **9** and **10** (Km for glucose is 120 μM). Owing to their structure, these inhibitors are likely to bind at the active site.

Concerning the two isomers **7** and **8**, the Lineweaver-Burk reciprocal plots (1/v versus 1/Glucose) intersect on the left of the 1/v axis, above the 1/G axis at any concentration of inhibitor. Replots of the 1/v axis intercept and slopes versus the inhibitor concentration are linear. These results signify that the nitro compounds act as mixed-type inhibitors with two inhibition constants K_i and K_{ii}; note that for compounds **1** and **8** neither can be confused with the value given by Coats *et al.*[22] (respectively 333 and 45 μM). The existence of different complexes was confirmed by kinetic measurements carried out without incubation of the inhibitor with the enzyme, (glucose, inhibitor and ATP being mixed together at zero time): in such a case, a competitive pattern (not shown) was observed.

(b) With respect to ATP

The corresponding reciprocal plots (1/v versus 1/ATP) give three different patterns: with compound **1**, with ortho substituted compounds **7** and **9**, and with meta substituted compounds **8** and **10**, respectively. (i) With compound **1**, the Lineweaver-Burk reciprocal plots yield parallel straight lines, the slopes of which are not changed by the concentration of the inhibitor.

The replots of 1/v axis intercepts are not a linear function of [I], providing evidence for a partially uncompetitive inhibition by this compound with respect to ATP; this implies that the ternary E.I.ATP complex is catalytically active. The activity of this complex is confirmed when the reaction is followed through ADP formation, instead of glucose-6-phosphate formation. In the absence of glucose hexokinase leads, in the presence of 10 mM of compound **1**, to ADP. (ii) With compounds **7** and **9**, the Lineweaver-Burk reciprocal plots intersect on the 1/ATP axis at any inhibitor concentration; both replots (slopes versus [I] and 1/v axis intercepts versus [I]) are parabolic up; consequently, the limits (which allow the determination of K_i and the β value in the expression Km.ATP/β.Vm) are difficult to obtain. This partially non-competitive inhibition accounts for a system where the inhibitor competes with glucose, but allows ATP to bind, leading in that case to the formation of one or several productive ternary E.I.ATP complexes. Using kinetic method B in the assay, ADP formation can be demonstrated. However, other phosphorylated products can be obtained (see below), as in the previous case for compound **1**. (iii) with compounds **8** and **10**, the reciprocal plots are non-linear. The plots arise close to the 1/v axis for increasing concentrations of the inhibitor. The kinetic measurements made in the absence of the glucose with inhibitors used as substrates, and by following ADP formation, indicate the presence of productive ternary complexes.

NMR Spectroscopic Studies

Inhibition studies with respect to the cofactor ATP performed with the different compounds indicate that in all cases catalytically active complexes are formed, since ADP production is observed. This may result from different processes; either from a phosphorylation of the inhibitor which can behave as an alternative substrate, since there is a free OH group at position 6, or from an ATPase activity of hexokinase, since such an activity has been demonstrated.[25,26]

Large scale experiments were therefore run in NMR tubes. Results are given in Table V. They indicate that in the presence of a large excess of inhibitor (10 mmoles) the ATP-Mg complex (20 μmoles), which is stable in the absence of hexokinase over a long period of time, undergoes in the presence of the enzyme a reaction leading only to three new phosphorylated compounds ADP-Mg (δ −9 and −5 ppm), inorganic phosphate (δ +2.5 ppm) and also AMP (δ +3.6 ppm) identified by comparison with

TABLE V ^{31}P NMR spectroscopy. Relative percentages of the phosphorylated compounds present after incubation of HK with inhibitors as substrate, in the absence of glucose. The chemical shift for 6-Phosphoglucosamine is +4.1 ppm

Compounds	%ATP	%ADP	%Pi	%AMP
HK+ATPMg	94.2	2.5	2.4	—
Xylose	93.1	3.5	3.3	—
OTG	87.1	6.6	4.7	1.6
1 phenyl	88.9	6.2	5.9	—
7 *o*-NO_2	85.1	7.4	6.1	1.3
8 *m*-NO_2	91.1	4.9	3.9	0.5
9 *o*-NH_2	93.6	4.3	1.0	2.0
10 *m*-NH_2	86.4	6.9	4.2	2.4

an authentic sample; the corresponding chemical shifts are in accordance with data from the literature.[27] In no case is a phosphorylated glucosamine formed and therefore inhibitors do not behave as pseudo-substrates. Concerning AMP, it can be observed that it is formed in low but significant quantities. It was verified that AMP does not result from a partial hydrolysis of ADP catalyzed by hexokinase.

DISCUSSION

As the identity of the current rebuilt structure of yeast hexokinase with the sequence initially inferred by Steitz is only 30%, this rebuilding of the structure by inserting the proper amino-acid sequence in the X-ray structure was required to define the actual interactions between the enzyme and the substrate glucose or the OTG inhibitor; however it is stressed that the geometry of the X-ray structure was retained. The analysis of the closed and open rebuilt structures thus obtained is in agreement with results from the literature: (i) in the close structure, it is seen that the two residues Ser 138 and Asp 191 (previously referred to as Asp 189) remain in close vicinity to the hydroxyl at position 6 of the glucose. This result is in agreement with the glucose phosphorylation process by hexokinase, since these two residues participate in the catalysis by transferring the γ phosphoryl from ATP to this hydroxyl group of glucose. Note that for mammalian Hexokinase I in the mutant S138A, this activity is suppressed.[28] (ii) the importance of the interactions between the hydroxyl at position 3 of the glucose and the protien, as indicated by the rebuilding, can account for the low affinity of glucose analogues bearing a substituent at this positon.[29] (iii) conversely, in the open structure of the OTG-hexokinase complex, only

Asp 191 on the large lobe of the protein remains in the vicinity of the 6-OH group, whereas the residue Ser 138 moves further, out of Van der Waals radii contact. (iv) certain non-phosphorylable sugars capable of binding to the enzyme at the specific glucose site, D-xylopyranose and D-lyxopyranose, promote a labilization of ATP[30] and the residue Ser 138 is phosphorylated.[31] This result is in accordance with the proximity of this residue with the 6-OH group in glucose in the catalytically active closed form, found by the modeling. The rebuilt structure of HK is in agreement with the main features concerning the binding of glucose or analogues at the active site.

Some confidence can therefore be given to the model which allows determination of the nature of residues present near the aromatic ring in the hexokinase-OTG complex. Two residues Glu 249 and Gln 278, appear located in the vicinity of the ortho and meta positions of the aromatic ring (2 to 3 Å) and no contact with para position is visible (Table I).

Other significant results from the HK-OTG interactions analysis revealed by the structure rebuilding, concern the NH–CO group and the CH_3 group in the inhibitor: the NH–C=O group gives a tight amide–amide interaction with the backbone of the protein at Ph 139 and the importance of this amide bond has previously been mentioned on the basis of experimental data. Without this amide bond, the inhibition effect on yeast hexokinase is dramatically decreased i.e. the N-anysilidene glucosamine has an inhibition constant in the range of 7 mM.[32] The methyl group of OTG is oriented towards the more hydrophobic Gln 278 residue of the protein which gives a more favorable interaction than that which would result from being in the vicinity of Glu 279 (Figure 2).

This modeling described here led to the design of other inhibitors bearing a substituent on the aromatic ring able to interact with Gln 278 and Glu 249 residues. To have inhibitors with stronger affinities, different structures were investigated, (i) those bearing H-bond donating groups (NH_2), (ii) bearing H-bond accepting groups (Br and NO_2) and (iii) a group able to promote both interactions (CH_3–NH–C=O). Types (i) and (ii) were expected to interact with Glu 249, and type (iii) with Gln 278.

The IC50 values in Table IV indicate that the carboxyl group (compound **5**) has no affinity likely due to repulsive interactions between anionic forms and the bromo and *N*-acetyl amido compounds have no affinity or reduced affinity respectively due possibly to steric hindrance. Conversely, the derivatives with a nitro and amino substituent at the ortho or meta position improve affinities, particularly when these substituents are attached in the ortho position. The distance between the nitrogen atom

and this residue seems to be critical since with the pyrazine ring, instead of the anilino ring, no interaction is observed.

It should also be noted that compounds **7** to **10** largely exist in the α-anomeric form, (see synthesis in Material and Method) likely due to an interaction between the OH group at postion 1 in the α-epimer and the NH group of the amide bond in the inhibitor. The binding is therefore likely obtained with a rather restricted conformation of the inhibitor.

Subsequently a kinetic study of these different inhibitors allowed the determination of their kinetic behaviour and the corresponding inhibition constants; corresponding values in Table IV indicate significant values (K_i/K_m ratios in the range of 1.5 to 3) for compounds **9** and **10**, but are rather far from the value given by Coats *et al.* for compounds **1** and **9** ($K_i < K_m$). This detailed kinetic analysis reveals other interesting features concerning hexokinase.

Firstly, inhibition regarding glucose indicates two different patterns: competitive and mixed type inhibitions. The mixed type inhibition is of particular interest in the relation to the mechanism of yeast hexokinase where several glucose-hexokinase complexes have been suggested, corresponding to different conformations of the enzyme;[24] by the same token, it can also be considered that several inhibitor-hexokinase complexes exist and are responsible for the mixed type process. This scheme is confirmed by the fact that this mixed type inhibition is transformed into a competitive pattern when the incubation of the inhibitor with the enzyme is suppressed. In these conditions this means that a single form of the enzyme interacts with the inhibitor giving a single EI complex type. During such a short interaction time between the enzyme and the inhibitor, no conformational change, induced by the glucose analogue binding to form several isomeric complexes, occurs or is kinetically significant. Secondly, the inhibition study with regard to ATP also gives different patterns which indicates that in all cases, ternary HK-Inhibitor-ATP complexes exist and are productive. This means that the presence of these glucose analogues at the active site does not prevent ATP binding, a result compatible with conclusions drawn from the "hypothetical model" for the OTG-HK complex. From a kinetic point of view, these glucose analogues can be considered as alternative substrates; this observation is confirmed by inhibition studies of ATP using method B, where ADP production was observed.

The NMR study reveals that these glucose analogues are not structurally alternative-substrates since no phosphorylation is observed at position 6 and therefore ADP production has to be accounted for by another reaction. As an ATPase activity of yeast hexokinase has previously been

mentioned, this activity was observed by the NMR technique: not only was ADP but also, to a low but significative amount, AMP apparent. This result indicates that within the ternary HK-I-ATP-Mg complex, a water molecule activated by Glu 249 which remains in the open form close to the 6-OH group and therefore to the γ-phosphate ATP group, promotes a partial hydrolysis of the cofactor, the P–O bond breaking being also observed to a lower extent between the α- and β- phosphate groups.

Finally the question of the role of Ser 138 in the hexokinase mechanism should be addressed. As indicated above, the modeling of the open form (in the absence of glucose) shows that only Glu 249 remains close to the 6-OH group, Ser 138 being further removed; in such conditions, only an ATPase activity is observed. On the contrary, in the close conformation, where only the phosphorylatin process occurs, the role of Ser 138 must be to keep away the water molecule responsible for ATP hydrolysis.

Other work is in progress for the design of inhibitors for hexokinase from different sources, particularly from parasites where glycolysis plays an essential role as a unique energy source. The present work indicates that such glucose analogues may act not only by blocking the enzyme in the phosphorylation process, but also by ATP depletion in promoting ATP hydrolysis. It is noteworthy that the highest ATP hydrolysis fraction is obtained with the glucose analogues having the best affinities.

References

[1] Willson, M., Callens, M., Kuntz, D.A., Périé, J. and Opperdoes, F.R. (1993) *Mol. Biochem. Parasitol.*, **59**, 201–210.
[2] Willson, M., Lauth, N., Périé, J., Callens, M. and Opperdoes, F.R. (1994) *Biochemistry*, **33**, 214–220.
[3] Potsma, P.W. and Lengerler, J.W. (1985) *Microbiol. Rev.*, **49**, 232–239.
[4] Bisson, L.F. and Fraenkel, D.F. (1983) *Proc. Natl. Acad. Sci. USA*, **80**, 1730–1734.
[5] Visser, N. and Opperdoes, F.R. (1980) *Eur. J. Biochem.*, **103**, 623–632.
[6] Périé, J., Alric, I., Blonski, C., Gefflaut, T., Lauth de Viguerie, N., Trinquier, M., Willson, M., Callens, M. and Opperdoes, F.R. (1994) *Pharmac. Ther.*, **60**, 347–365.
[7] Swarup, G. and Kenkare, U.W. (1980) *Biochemistry*, **19**, 4058–4064.
[8] Schirch, D.M. and Wilson, J.E. (1987) *Arch. Biochem. Biophys.*, **254**, 385–396.
[9] Magnani, M., Stocchi, V., Serafini, G. and Chiarantini, L. (1988) *Biochem. Biophys. Acta*, **954**, 336–343.
[10] Mehta, A.M., Jarori, G.K. and Kenkare, U.W. (1988) *Biol. Chem.*, **263**, 15492–15498.
[11] Akerfeldt, K.S. and Bartlett, P.A. (1991) *J. Org. Chem.*, **56**, 7133–7144.
[12] Alric, I., Willson, M. and Périé, J. (1991) *Phosphorus and Sulfur*, **56**, 71–80.
[13] Bennett, W.S. and Steitz, T.A. (1980) *J. Mol. Biol.*, **140**, 183–209.
[14] Bennett, W.S. and Steitz, T.A. (1980) *J. Mol. Biol.*, **140**, 211–230.
[15] Steitz, T.A., Fletteik, R.J., Anderson, W.F. and Anderson, C.M. (1976) *J. Mol. Biol.*, **104**, 197–222.
[16] Anderson, C.M., Stenkamp, R.E., McDonald, R.C. and Steitz, T.A. (1978) *J. Mol. Biol.*, **123**, 207–219.
[17] Maley, F. and Lardy, H.A. (1955) *J. Biol. Chem.*, **214**, 765–773.

[18] Perie, J., Alric, I., Blonski, C., Chauvière, G., Lauth, N., Willson, M., Albuquerque, C., Gefflaut, T. and Trinquier, M. (1993) *Actual. Chim. Ther.*, **20**, 111–148.
[19] Steitz, T.A., Anderson, W.F., Fletterick, R.J. and Anderson, C.M. (1977) *J. Biol. Chem.*, **252**, 4494–4500.
[20] Stachelek, C., Stachelek, J., Swan, J., Boistein, D. and Konisgberg, W. (1986) *Nucleic Acid Res.*, **14**, 945–963.
[21] Fothergill-Gilmore, L. and Michels, P.A.M. (1993) *Prog. Biophys. Mol. Biol.*, **2**, 105–177.
[22] Coats, E.A., Skau, K.A., Caperelli, C.A. and Solamacha, D. (1993) *J. Enz. Inhibit.*, **6**, 271–282.
[23] Alric, I. (1991) *Thesis*, no. 1026, Paul Sabatier University, Toulouse France.
[24] Rose, I.A. (1995) *Meth. Enzymol.*, **249**, 315–340.
[25] Kaji, A., Trayser, K.A. and Colowick, S.P. (1961) *Fed. Proc.*, **20**, 233–239.
[26] Zewe, V., Fromm, M. and Fabiano, R. (1964) *J. Biol. Chem.*, **239**, 1625–1634.
[27] Tebby, J.C. and Glonek, T. (1991) *Handbook of Phosphorus-31 NMR Data* (J. Tebby (ed.)). CRC press; Boca Raton, Fl.
[28] Baijal, M. and Wilson, J.E. (1992) *Arch. Biochem. Biophys.*, **298**, 271–278.
[29] Sols, A., De La Fuente, G., Villar-Palasi, C. and Asensio, C. (1958) *Biochem. Biophys. Acta*, **30**, 92–101.
[30] De la Fuente, G., Lagunas, R. and Sols, A. (1970) *Eur. J. Biochem.*, **16**, 226–233.
[31] Menezez, L.C. and Pudles, J. (1977) *Arch. Biochem. Biophys.*, **178**, 34–42.
[32] Trinquier-Dinet, M. (1995) *Thesis*, no. 126, Paul Sabatier University, Toulouse France.
[33] Lipmar, D.J. and Pearson, W.R. (1985) *Science*, **227**, 1435–1446.
[34] Krauslis, P.J. (1991) *J. Appl. Crystallogr.*, **24**, 946–952.